

# The effect of zinc oxide nanostructure on the performance of hybrid polymer/zinc oxide solar cells

A.M Peiró<sup>a</sup>, P. Ravirajan<sup>b,c</sup>, K. Govender<sup>d</sup>, D.S. Boyle<sup>d</sup>, P.O'Brien<sup>d</sup>, D.D.C. Bradley<sup>b</sup>,  
J. Nelson<sup>b</sup> and J.R. Durrant<sup>a</sup>

<sup>a</sup>Centre for Electronic Materials and Devices, Dept. of Chemistry, Imperial College London,  
Exhibition Road, London SW7 2AZ, U.K.

<sup>b</sup>Centre for Electronic Materials and Devices, Dept. of Physics, Imperial College London,  
Prince Consort Road, London SW7 2BW, U.K.

<sup>c</sup>Dept. of Physics, University of Jaffna, Sri Lanka

<sup>d</sup>The Manchester Materials Science Centre and Department of Chemistry,  
University of Manchester, Oxford Road, Manchester, UK M13 9PL.

## ABSTRACT

Solar cells fabricated from composites of conjugated polymers with nanostructured metal oxides are gaining interest on account of the stability, low cost and electron transport properties of metal oxides. Zinc oxide (ZnO)/polymer solar cells are promising compared to other metal oxide/polymer combinations, on account of the possibility of low temperature synthesis, as well as the potential for controlling interface morphology through simple processing from solution. Here, we focus on the effect of surface morphology of ZnO films on photovoltaic device performance. We have successfully grown ZnO nanorods standing almost perpendicular to the electrodes on a flat, dense ZnO “backing” layer. We studied structures consisting of a conjugated polymer in contact with three different types of ZnO layer: a flat ZnO backing layer alone; ZnO nanorods on a ZnO backing layer; and ZnO nanoparticles on a ZnO backing layer. We use scanning electron microscopy, steady state and transient absorption spectroscopies and photovoltaic device measurements to study the morphology, charge separation and recombination behaviour and device performance of the three types of structures. We find that charge recombination in the structures containing vertically aligned ZnO nanorods is remarkably slow, with a half life of over 1 ms, over two orders of magnitude slower than for randomly oriented ZnO nanoparticles. A photovoltaic device based on the nanorod structure which has been treated with an amphiphilic dye before deposition of poly(3-hexyl thiophene) (P3HT) polymer shows a power conversion efficiency over four times greater than for a similar device based on the nanoparticle structure. The best ZnO nanorods: P3HT device yields a short circuit current density of  $2 \text{ mAcm}^{-2}$  under AM1.5 illumination ( $100 \text{ mWcm}^{-2}$ ) and peak external quantum efficiency over 14%, resulting in a power conversion efficiency of 0.20%.

**Keywords:** hybrid solar cells, photovoltaics, ZnO, rods, metal oxide, polymer, P3HT, transient absorption.

## 1. INTRODUCTION

In recent years, there has been heightened interest in organic solar cells on account of their range of potential applications, their ease of fabrication and potentially low cost compared to inorganic solar cells<sup>1-3</sup>. Particularly promising are hybrid solar cells, made from composites of conjugated polymers with nanostructured metal oxides, in which the polymer serves the function of both light absorber and hole-conductor and the metal oxide acts as the electron transporter. External quantum efficiencies of over 40 % have been achieved in photovoltaic devices based on conjugated polymers combined with metal oxide nanoparticles or nanoparticle films<sup>4,5</sup>.

In this study, we focus on a strategy to increase the charge separation yield and control recombination kinetics in these structures. Our strategy has been to grow ZnO nanorods perpendicular to a dense ZnO ‘backing layer’, as a means to provide a direct and ordered path for photogenerated electrons to the collecting electrode and to control charge recombination losses. The backing layer serves to prevent unwanted hole transfer from the polymer to the conducting glass substrate. We have assessed different synthetic routes for both the ZnO backing layer and the ZnO rod preparation.

The ZnO rod structure was filled with regioregular poly(3-hexylthiophene) polymer, P3HT, which was selected as the light absorbing and hole-transporting component. We show that charge recombination in the structure containing vertically aligned ZnO nanorods is remarkably slow, and is over two orders of magnitude slower than for randomly oriented ZnO nanoparticles. We also find that photovoltaic devices based on the nanorod structure with poly(3-hexyl thiophene) show a power conversion efficiency over four times greater than for a similar devices based on the nanoparticle structure.

## 2. EXPERIMENTAL

### 2.1 Sample fabrication.

Samples were prepared on indium tin oxide coated glass substrates (ITO,  $\sim 1 \text{ cm}^2$ , 10-15  $\Omega/\text{square}$ ), which were first cleaned by ultrasonic agitation in acetone and isopropanol and dried under nitrogen flow.

**Backing layer preparation:** Different methods were investigated in order to prepare ZnO layers that prevented direct contact of polymer with ITO.

*Sol-gel dip-coating method:*<sup>6</sup> A solution of zinc acetate dihydrate in n-propanol ( $120 \text{ cm}^3$ ) was heated under reflux conditions ( $130 \text{ }^\circ\text{C}$ , 20 min). The mixture was allowed to cool to ambient temperature before rapid addition of tetramethylammonium hydroxide (25% in MeOH,  $36 \text{ cm}^3$ ) to yield a transparent nanoparticulate ZnO coating sol, which could be concentrated further by removal of solvent using a rotary evaporator. Different initial concentrations of the ZnO precursor were essayed (0.1M to 0.5M), in order to obtain films of different thicknesses. Films were prepared by dip-coating substrates in the sol and sintering in a furnace at  $400 \text{ }^\circ\text{C}$  for 2 min. Heat treatment of the samples at  $400^\circ\text{C}$  for 20 min was also essayed.

*Spin-coating method:* Spin-coating methods involved the preparation of 40 nm films by five consecutive deposition processes using three methods, adapted from the literature:<sup>7-9</sup> 1) a solution of zinc acetate (0.6 M) in dimethylformamide, 2) a solution of zinc acetate (0.20 M) in methanol, 3) a solution of zinc acetate (0.35 M) and monoethanolamine(0.35 M) in 2-methoxyethanol. All solutions were left stirring overnight at room temperature before use, filtered and spin-coated at 3000 rpm for 30 s. Films were dried at  $70 \text{ }^\circ\text{C}$  for 10 min and calcined at  $450 \text{ }^\circ\text{C}$  for 20 min. Solutions of Method 2 were also spin-coated at different speeds, in order to obtain different thicknesses, ranging from 70 nm to 30 nm.

*Spray-pyrolysis method:* Precursor solutions containing zinc acetate (0.978-1.756 g) in 20 ml of methanol or dimethylformamide were prepared for the spray-pyrolysis method. Deposition took place at  $400^\circ\text{C}$ . After deposition, films were calcined at  $400^\circ\text{C}$  for 20 min, resulting in ZnO films of thickness about 50-70 nm. Best compact layers were obtained with the more concentrated solutions, using methanol as a solvent.

**ZnO particles preparation:** ZnO particles were prepared by heating 0.1 M zinc nitrate ( $\text{Zn}(\text{NO}_3)_2 \cdot 6\text{H}_2\text{O}$ ) aqueous solution (pH 5, adjusted with nitric acid) in the presence of 0.1 M triethanolamine, following similar procedure to that described in Ref.[10a]. The synthesis was conducted in tightly stoppered glass flasks, using 250 ml of solution, unstirred, and heated at  $100 \text{ }^\circ\text{C}$  for 24 h. After this time, precipitation of ZnO particles was observed. After cooling down at room temperature, the supernatant water was extracted. The precipitate was centrifuged and washed with distilled water to remove any residual salt. This process was repeated four times. Finally, the powder was dried overnight at room temperature, followed by drying at  $100 \text{ }^\circ\text{C}$  for 4 h. A ZnO paste was prepared with these particles, following similar procedure to that described in Ref [10b]. ZnO powder (3 g) was mixed with 0.1 ml of acetylacetone. To this mixture, 1 ml of  $\text{H}_2\text{O}$  with acetylacetone (10/1) in 0.1 ml portions was added, while grinding continuously. Then, 0.1  $\mu\text{l}$  of Triton-X were added, while stirring with a magnetic stirrer, followed by 2 ml of  $\text{H}_2\text{O}$ . The suspension was stirred for 1 day. The obtained paste was spin-coated onto the ZnO dense films, after the appropriate amount of water was added to obtain the desired film thickness (500-700 nm). Finally, the film was calcined at  $400^\circ\text{C}$  for 20 min, to improve particle cohesion.

**ZnO rods preparation:** Different methods were investigated in order to prepare ZnO rods onto ZnO backing layers.

*Zn Acetate/ $\text{NH}_3$ / $\text{HCHO}$  and Zn nitrate/HMT deposition methods* are described in Ref [6]. Briefly, the first method uses zinc acetate precursor ( $0.025 \text{ mol dm}^{-3}$ ), formaldehyde ( $\text{HCHO}$ ,  $0.016 \text{ mol dm}^{-3}$ ) and ammonia ( $\text{NH}_3$ ,  $0.0083 \text{ mol dm}^{-3}$ ), at pH 6.9,  $90 \text{ }^\circ\text{C}$  for 2 h, and the second method, zinc nitrate precursor ( $0.025 \text{ mol dm}^{-3}$ ) and hexamethylenetetramine (HMT,  $0.025 \text{ mol dm}^{-3}$ ), at pH 5,  $90 \text{ }^\circ\text{C}$  for 2 h.

*ZnSO<sub>4</sub>/NH<sub>4</sub>Cl method:*<sup>11</sup> Briefly, a stock solution of zinc sulphate ( $\text{ZnSO}_4 \cdot 7\text{H}_2\text{O}$ , 0.02 M) and ammonium chloride ( $\text{NH}_4\text{Cl}$ , 0.6M) was prepared using  $\text{H}_2\text{O}$  as a solvent. This solution was further diluted to 0.01 M in  $\text{Zn}^{2+}$  and then, the pH

was adjusted to 11.00 with sodium hydroxide (NaOH). ZnO rod deposition onto the ZnO dense layers took place at 60 °C for 3-24 h. Following deposition, substrates were rinsed and sonicated in distilled water, and finally dried under N<sub>2</sub> flow.

**Dip-coating step:** The metal oxide films were immersed overnight in a solution of poly(3-hexylthiophene) (P3HT) in chlorobenzene (C<sub>6</sub>H<sub>5</sub>Cl, 2 mg/ml) or in a 0.3 mM solution of amphiphilic polypyridyl ruthenium complex, cis-RuLL'(SCN)<sub>2</sub> (L=4,4'-dicarboxylic acid-2,2'-bipyridine, L'=4,4'-dinonyl-2,2'-bipyridine) (Z907)<sup>12</sup> in acetonitrile:tert-butanol (1:1 vol%) at 100 °C. The dip-coated film was then “wiped” by a quick blow with dry nitrogen gas and heated at 50 °C in air.

**Spin-coating step:** 80 nm polymer layer was deposited onto the films by spin-coating from a polymer solution in C<sub>6</sub>H<sub>5</sub>Cl (15-20 mg/ml) at 2000 rpm.

**Device preparation:** Devices were prepared by spin-coating a layer of poly(ethylene dioxythiophene) doped with poly(styrene sulfonic acid) (PEDOT:PSS) onto the spin-coated polymer films. Au contact was deposited on top. The active area of each device was ~ 4.2 mm<sup>2</sup>. Previous studies have demonstrated that device performance of hybrid PPV-based polymer/metal oxide cells is improved by introducing a layer of PEDOT:PSS under the top contact.<sup>13</sup> In this study using P3HT polymer, we have adopted a slightly different procedure, in which isopropanol (1:1 or 50 % volume) is incorporated into the PEDOT solution prior to spin coating on the P3HT / ZnO rods devices. The PEDOT:PSS solution was first ultrasonicated for 15 minutes and then heated at 90 °C for 15 minutes. The solution was filtered with a 0.45 μm filter and 50 % (volume) of IPA was then added into the PEDOT solution. Finally, the resulting solution was spin coated onto the dried semiconducting polymer layer.

## 2.2 Electrical measurements

Samples were housed in a home built sample holder with a quartz window for electrical measurements.<sup>14</sup> Current-voltage measurements were obtained using a ScienceTech solar simulator and AM 1.5 spectral filter. Calibration of the light intensity was achieved by using band-pass filters of known transmission combined with a silicon photodiode with independently certified spectral response, calibrated at the ISE-Fraunhofer Institut in Freiburg Germany. The lamp intensity was adjusted to give close (±10 %) agreement with theoretical one sun AM 1.5 intensity over spectral region of the dye optical absorption (450 – 700 nm).

## 2.3 Optical measurements

Transient absorption characterizations were undertaken as reported previously.<sup>15,16</sup> Transient absorption studies employed low excitation density excitation (540 nm excitation, < 1 ns pulse duration, 0.8 Hz, intensity ~30 μJ/pulse/cm<sup>2</sup>). The excitation wavelength (540 nm) corresponded to the absorption maximum of P3HT polymer and the probe wavelength (900 nm) to the absorption maximum of the P3HT<sup>+</sup> polarons.

# 3. RESULTS

## 3.1 Schematic of device structure and active layer

Figure 1(a) shows a schematic of our device structure. The figure shows two electrodes (ITO conducting glass and Au), with the active layer (containing the polymer and the metal oxide) lying between them. Generated electrons move to the ITO contact through a ZnO hole blocking layer (“backing layer”) and holes move to the Au electrode through a PEDOT:PSS electron blocking layer.

The achievement of working devices is possible through the optimisation of different cell components such as the “backing layer”, the design of the active layer and the choice of polymer. Figures 1(b) - (d) show the three active layer designs that have been addressed in this work.

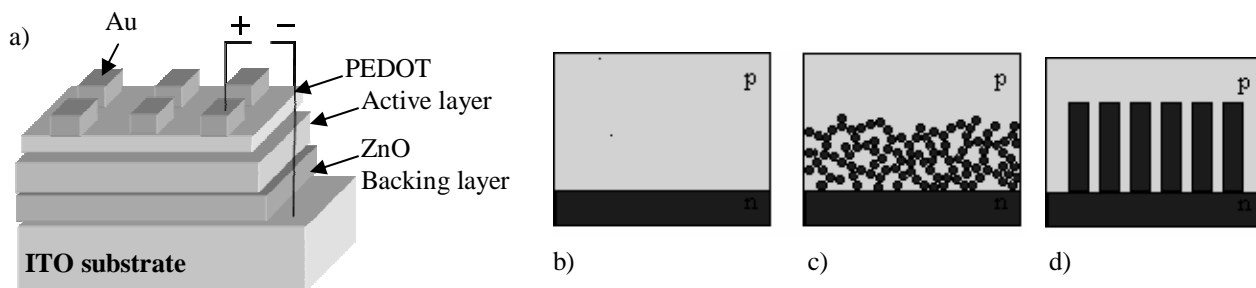


Figure 1. Schematic of a) the device structure and b)-d) the designs of active layers addressed in this work. Figure b) corresponds to a dense ZnO backing layer in contact with a polymer film (bi-layer structure), c) consists on a porous nanocrystalline structure deposited on top of a dense backing layer, where the structure is filled with the polymer, and d) shows a columnar structure grown on top of a dense backing layer, where the polymer is interpenetrating the structure.

### 3.2 Optimisation of compact ZnO backing layers

As shown in Figure 1, in the device structures addressed in this work, a dense layer is needed in order to prevent direct contact between the polymer and the ITO substrate, and it is referred to as a “hole-blocking layer” or “backing layer”. Several methods (dip-coating, spin-coating and spray-pyrolysis) were essayed in order to prepare compact ZnO films which would serve both as backing layer and templates for the growth of ZnO rods (see experimental section for details on the approaches addressed). Figure 2 (a) and (b) show Scanning Electron Microscopy (SEM) images of ZnO backing layers prepared by the dip-coating and spray-pyrolysis methods, respectively. The spray-pyrolysis method provided better compact films. This method was optimised by assessing the effect of different concentrations of the ZnO precursor and of different solvents. Transparent and well-adhered films were obtained from zinc acetate solutions in methanol. These films showed the best diode behaviour at dark, when incorporated into devices with the structure shown in Figure 1(b) (bi-layer devices). Figure 2 (c) compares the current density-voltage (J-V) characteristics of a bi-layer device made with these ZnO compact layers with those of a bi-layer device made from a standard compact TiO<sub>2</sub> backing layer, prepared by the same method (used in our previous work on hybrid solar cells).<sup>14</sup> Devices containing spray-pyrolysis ZnO layers showed higher J<sub>sc</sub> and lower V<sub>oc</sub> than devices fabricated with spray-pyrolysis TiO<sub>2</sub> dense layers. In the dark, ZnO films showed higher dark current, which could be assigned to hole injection through an imperfectly compact backing layer.

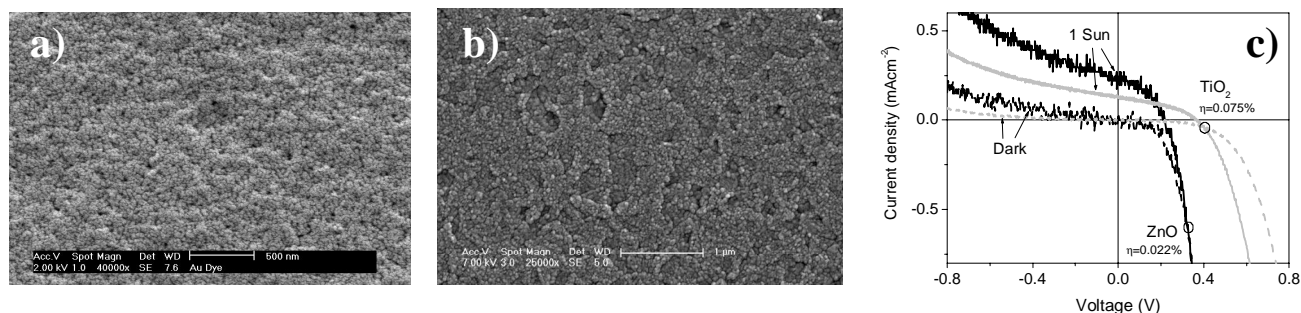


Figure 2. SEM images of ZnO backing layers prepared by a) dip and b) spray-pyrolysis methods and c) J-V curves (1 Sun and dark) of ZnO spray-pyrolysis and TiO<sub>2</sub> compact layers. Film thickness was 50 nm in all cases. For the devices, P3HT polymer was spin-coated on top of the backing layers and PEDOT:PSS and Au were deposited on top of the polymer. The device structure is ITO/ZnO backing layer/P3HT<sup>spin</sup>/PEDOT:PSS/Au. Scale bars in a) and b) are 500 nm and 1 μm, respectively.

Spray-pyrolysis ZnO layers were selected due to their J-V characteristics for their use as hole-blocking layers in further experiments involving the growth of ZnO rods. TiO<sub>2</sub> compact backing layers were also assessed for this function. However, ZnO rods grown on them showed non-homogeneous diameter sizes and formed patches of aggregates, most probably due to structural mismatch. Additionally, bi-layer devices made with these TiO<sub>2</sub> backing layers generated very low current.

### 3.3 Evaluation of different synthetic routes for ZnO rods preparation.

ZnO particles with diameter in the range of 70-150 nm were prepared as described in the literature (see section 2.1 for details). These particles were deposited onto the spray-pyrolysis ZnO backing layers to form a porous structure, which was filled with polymer (as schematic Figure 1(c)). Film thicknesses ranged from ca. 500 – 1000 nm, depending on the spin-coating conditions and were adjusted so that they were comparable to the ZnO rod films thicknesses.

Different soft-solution chemical routes were essayed for the preparation of ZnO rods of different dimensions. Figure 3 shows some examples of the rods prepared on the ZnO spray-pyrolysis films. All methods were performed at low temperature and atmospheric pressure (see section 2.1 for details). These structures were incorporated into devices, using P3HT polymer as hole conductor. As shown in Figure 4, only devices prepared by the  $\text{ZnSO}_4/\text{NH}_4\text{Cl}$  method showed acceptable dark current behaviour without large shunt effects. For all other preparation methods, the dark current was considerably high, indicating that the ZnO backing layer was not compact enough and it might have been damaged during the growth of the ZnO rods. This fact could be ascribed to partial dissolution of the ZnO backing layer due to the higher reaction temperature ( $90^\circ\text{C}$ ) used for the fabrication of structures in Figure 3 (a) and (c), compared to the growth at  $60^\circ\text{C}$  of the structures in Figure 3 (b).

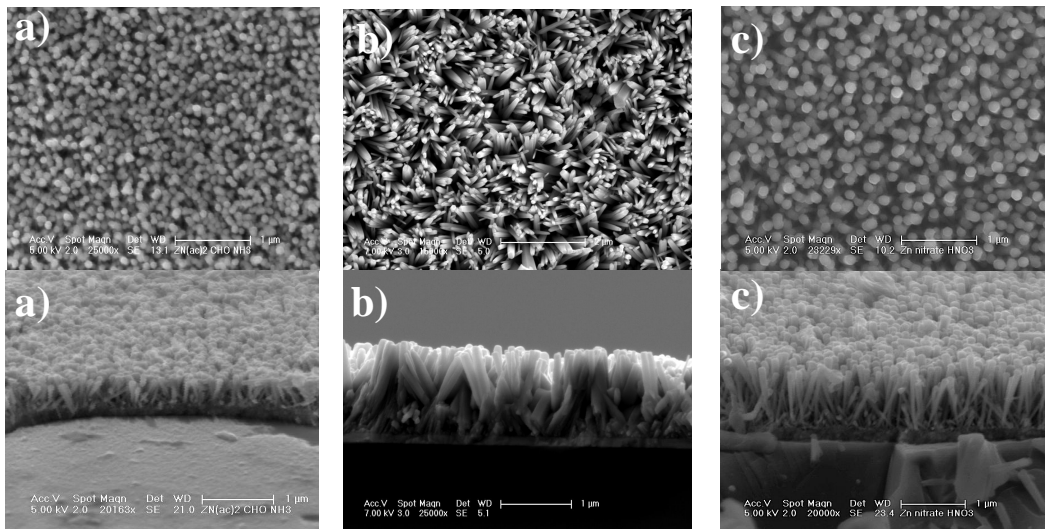


Figure 3. SEM micrographs of ZnO films with different microstructure. Images a)-c) correspond to ZnO rods grown onto ZnO backing layers by different methods: a) Zinc acetate/ $\text{NH}_3$ /HCHO method, b)  $\text{ZnSO}_4/\text{NH}_4\text{Cl}$  6 h method and c) Zinc nitrate/HMT method. Dimensions are: a) diameter  $\sim 85$  nm, length  $\sim 325$  nm (aspect ratio  $\sim 4$ ); b) diameter 60-100 nm, length 550-1000 nm (aspect ratio  $\sim 10$ ) and c) diameter  $\sim 135$  nm, length  $\sim 910$  nm (aspect ratio  $\sim 7$ ). Scale bars are 1  $\mu\text{m}$  in all figures, except b) top, where it is 2  $\mu\text{m}$ .

The method using  $\text{ZnSO}_4/\text{NH}_4\text{Cl}$  for ZnO rod growth was optimised by studying the effect of the reaction time on the morphological characteristics of the film. Different reaction times from 3 to 24 h were essayed for the rod growth. Rods prepared for longer reaction times were more homogeneous in length than the ones corresponding to shorter times but, in all cases, the length seemed to stabilise at ca. 1000 nm. This fact indicated that most of the ZnO precursor must have reacted after only a few hours. However, as Figure 5 shows, for long reaction times, deposition of star-like ZnO particles, mainly loose, also took place onto the ZnO rod films. These particles would have grown by homogeneous reaction in solution rather than heterogeneous reaction. Bath sonication was used in order to remove the loose particles from the ZnO rod ends, but this approach was not fully effective for some of the particles deposited after longer reaction periods. These ZnO deposits would hinder the charge collection at the Au electrode. For this reason, only films prepared for 3 to 6 h periods, which didn't show star-like deposits, were selected for device fabrication.

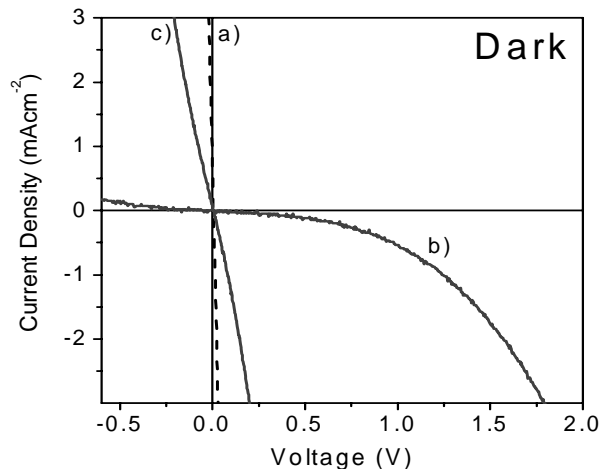


Fig. 4. Dark IV curves for devices made with ZnO rods prepared by different methods: a) Zinc acetate/ $\text{NH}_3$ /HCHO method, b)  $\text{ZnSO}_4/\text{NH}_4\text{Cl}$  6 h method and c) Zinc nitrate/HMT method. Samples were dip and spin-coated in P3HT polymer, PEDOT:PSS was spin-coated and Au was evaporated on top. Device structure: ITO/ZnO backing layer/ZnO rods/P3HT<sup>dip</sup>/P3HT<sup>spin</sup>/PEDOT:PSS/Au.

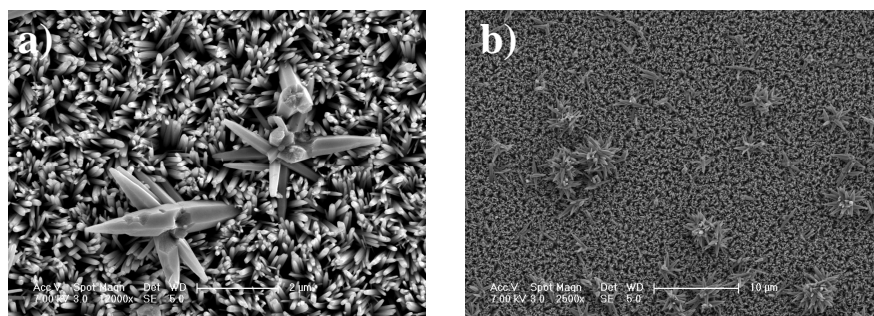


Figure 5. SEM images of ZnO rods films grown on spray-pyrolysis ZnO backing layer by the  $\text{ZnSO}_4/\text{NH}_4\text{Cl}$  method for 12 h. Well-adhered star-like ZnO crystals can be observed on top of the ZnO rod film. Magnification and scale bars: a) 12000x, 2  $\mu\text{m}$ ; b) 2500x, 10  $\mu\text{m}$ .

### 3.6 Optical and electrical measurements on samples with different active layer designs.

Our previous studies of polymer /  $\text{TiO}_2$  nanoparticle films have demonstrated that device performance improves by dip-coating the  $\text{TiO}_2$  film in polymer solution prior to spin-coating the polymer material. In our work in Ref [16], we have extended this approach to the use of an ambiphilic dye *cis*-RuLL'(SCN)<sub>2</sub> (L=4,4'-dicarboxylic acid-2,2'-bipyridine, L'=4,4'-dinonyl-2,2'- bipyridine), often referred to as Z907, for the dip-coating step. We have observed that the incorporation of a Z907 layer provides improved charge separation yield and helps reducing dark current. Details on the mechanisms involved can be found in Ref.[16]. All results presented in this section involve the use of Z907 dye in a dip-coating pre-treatment, as a route to improved device efficiencies.

Figure 6(a) shows the transient absorption signals of structures consisting of ZnO backing layer, ZnO backing layer/ZnO particles and ZnO backing layer/ZnO rods, dip-coated with Z907 dye before spin-coating the P3HT polymer layer. Slower recombination kinetics were observed for ZnO rods, compared to ZnO particles and compact ZnO films. This fact is tentatively assigned to better connectivity in the ZnO rods, compared to particles, allowing easier escape for electrons from ZnO/polymer interfacial recombination sites. It is furthermore apparent from Figure 6(a) that the ZnO rods result in a significant enhancement of charge separation yield relative to the compact ZnO film alone, consistent with the higher interfacial area of these rods for exciton dissociation.

Figure 6(b) shows the effect of ZnO layer morphology on the current-voltage characteristics of dye treated ZnO: P3HT devices incorporating different ZnO nanostructures. The figure shows that introducing ZnO nanorods or particles in the device structure increases  $J_{sc}$ , compared to bi-layer devices made with Z907:P3HT on dense ZnO backing layer, as expected due to the increased interfacial area. Devices incorporating rods show external quantum efficiency over 14 % at 550 nm.<sup>16</sup> Moreover, devices made with nanorods show the highest  $V_{oc}$  and  $J_{sc}$ , resulting in power conversion efficiency over four times greater than for similar devices made with nanoparticles. The higher  $V_{oc}$  is consistent with the slower recombination noted above (Figure 6a).

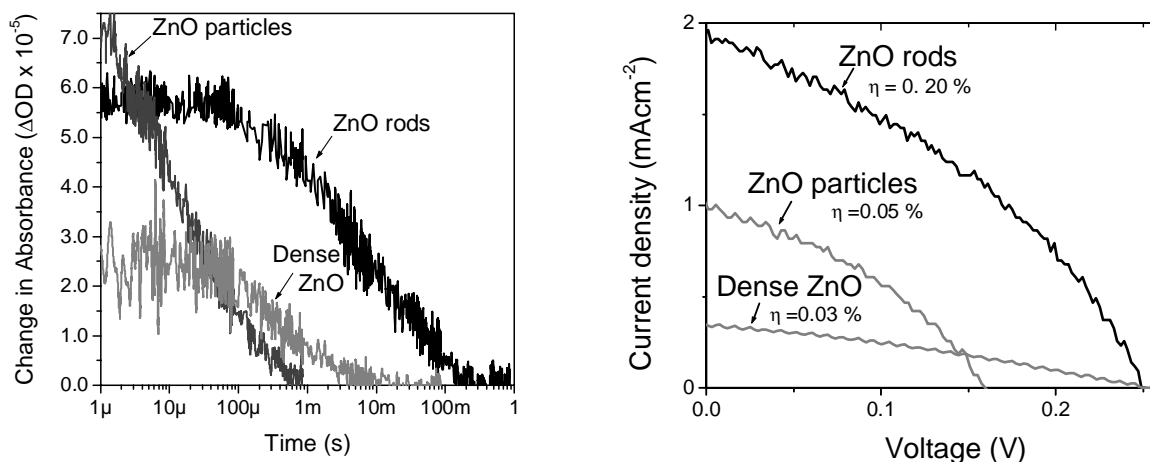


Figure 6. a) Photoinduced change in absorbance for structures containing ZnO backing layer only, ZnO particles and ZnO rods ( $ZnSO_4/NH_4Cl$  6 h), treated with Z907 dye and P3HT polymer. Sample structure: ITO/ZnO backing layer/ZnO rods or particles/Z907<sup>dip</sup>/P3HT<sup>spin</sup>. Pump  $\lambda$ : 540 nm, Probe  $\lambda$ : 900 nm, repetition rate: 0.8 Hz. b) Current density-Voltage curves of devices made with the same structures shown in a), after deposition of PEDOT:PSS and Au. Device structures: ITO/ZnO backing layer/ZnO rods or particles/Z907<sup>dip</sup>/P3HT<sup>spin</sup>/ PEDOT:PSS /Au.

#### 4. CONCLUSIONS

In conclusion, this work has dealt with the optimisation of different hybrid cell components, namely the dense backing layer and the design of the active layer. A spray-pyrolysis method, based on a zinc acetate solution in methanol, has been selected for the preparation of compact zinc oxide films. Several methods have been assessed for the preparation of ZnO rods onto these zinc oxide compact films, and best results have been obtained with a method using a zinc sulphate and ammonium chloride solution in water, at pH 11 for 3-6 h at 60 °C. Other methods essayed seemed to dissolve the zinc oxide backing layer during the rod formation. A comparison of the optical and electrical properties of hybrid ZnO :P3HT polymer structures containing ZnO backing layer alone, ZnO particles and ZnO rods, has shown that the structures containing rods present the slowest recombination kinetics (with a half life of ~ 6 ms, over two orders of magnitude slower than for ZnO nanoparticles) and the highest power conversion efficiency. These facts are tentatively assigned to better connectivity in the ZnO rods, compared to particles, allowing easier escape for electrons from ZnO/polymer interfacial recombination sites. Also, the significant enhancement of charge separation yield and  $J_{sc}$  for structures with ZnO rods relative to the compact ZnO film alone is assigned to the higher interfacial area available for the rods for exciton dissociation. The best ZnO nanorods: P3HT device yields a short circuit current density of  $2mAc_m^{-2}$  under AM1.5 illumination ( $100mWcm^{-2}$ ) and peak external quantum efficiency over 14 %, resulting in a power conversion efficiency of 0.20 %. These values are significantly lower than for the best polymer-fullerene solar cells. The low  $V_{oc}$  can be attributed partly to shunt losses due to imperfections of the dense ZnO layer, and the low  $J_{sc}$  to low charge separation efficiency due to the large film pore sizes (~ 100 nm) relative to the P3HT exciton diffusion length. We expect improved device performance can be obtained through the optimization of the blocking function of the dense ZnO layer and the dimensions of the ZnO rods.

## ACKNOWLEDGEMENTS

We are grateful to Merck Chemicals Ltd for providing the P3HT polymer used in this study. We would like to thank M.K. Nazeeruddin and M. Grätzel from the Laboratory for Photonics and Interfaces, Switzerland, for supplying Z907 dye. We acknowledge EPSRC and the Commission of the European Community (Project MOLYCELL Contract No. 502783) for their financial assistance. Ana M. Peiró acknowledges the Spanish *Secretaría de Estado de Universidades e Investigación del Ministerio de Educación y Ciencia* for a postdoctoral fellowship. We would like to thank Dr. Jessica E. Kroeze for assistance and Dr. Brian O'Regan for useful discussions.

## REFERENCES

1. M. Grätzel, "Photoelectrochemical Cells", *Nature*, **414**, 332-344, 2001.
2. C.J. Brabec, N.S. Sariciftci, J.C. Hummelen, "Plastic Solar Cells", *Adv. Func. Mat.*, **11**, 15-26, 2001.
3. J. Nelson, "Organic Photovoltaic Films", *Materials Today*, **5**, 20-27, 2002.
4. W. J. E. Beek, M. M. Wienk, R. A. J. Janssen, "Efficient Hybrid Solar Cells from Zinc Oxide Nanoparticles and a Conjugated Polymer", *Adv. Mater.*, **16**, 1009-1013, 2004.
5. P. Ravirajan, S. A. Haque, J. R. Durrant, H. J. P. Smit, J. M. Kroon, D. D. C. Bradley, J. Nelson, "Efficient charge collection in hybrid polymer/TiO<sub>2</sub> solar cells using poly(ethylenedioxythiophene)/polystyrene sulphonate as hole collector", *Appl. Phys. Lett.*, **86**, 143101, 2005.
6. K. Govender, D.S. Boyle, P.B. Kenway, P. O'Brien, "Understanding the factors that govern the deposition and morphology of thin films of ZnO from aqueous solution", *J. Mater. Chem.*, **14**, 2575-2591, 2004.
7. N.R.S. Farley, C.R. Staddon, L. Zhao, K.W. Edmonds, B.L. Gallagher and D.H. Gregory, "Sol-gel formation of ordered nanostructured doped ZnO films", *J. Mater. Chem.*, **14**, 1087-1092, 2004.
8. Y. Natsume and H. Sakata, "Zinc oxide films prepared by sol-gel spin-coating", *Thin Solid Films*, **372**, 30-36, 2000.
9. J. H. Lee, K.H. Ko, B.O. Park, "Electrical and optical properties of ZnO transparent conducting films by the sol-gel method", *J. Crystal Growth*, **247**, 119-125, 2003.
10. a) K. Westermark, H. Rensmo, H. Siegbahn, K. Keis, A. Hagfeldt, L. Ojamäe, P. Persson, "PES Studies of Ru(dcbpyH<sub>2</sub>)<sub>2</sub>(NCS)<sub>2</sub> Adsorption on Nanostructured ZnO for Solar Cell Applications", *J. Phys. Chem. B*, **106**, 10102-10107, 2002. b) L. Kavan, B. O'Regan, A. Kay, M. Gratzel, "Preparation of TiO<sub>2</sub> (anatase) films on electrodes by anodic oxidative hydrolysis of TiCl<sub>3</sub>", *J. Electroanal. Chem.*, **346**, 291-307, 1993.
11. S. Yamabi, H. Imai, "Growth conditions for wurtzite zinc oxide films in aqueous solutions", *J. Mater. Chem.*, **12**, 3773-3778, 2002.
12. P. Wang, S. M. Zakeeruddin, I. Exnar, M. Grätzel, "High efficiency dye-sensitized nanocrystalline solar cells based on ionic liquid polymer gel electrolyte", *Chem. Commun.*, 2972-2973, 2002.
13. a) P. Ravirajan, S. A. Haque, J. R. Durrant, D. D. C. Bradley, J. Nelson, "The effect of polymer optoelectronic properties on the performance of multilayer hybrid polymer/TiO<sub>2</sub> solar cells", *Adv. Func. Mat.* **15** (4), 609-618, 2005. b) P. Ravirajan, D. D. C. Bradley, J. Nelson, S. A. Haque, J. R. Durrant, H. J. P. Smit, J. M. Kroon, "Efficient charge collection in hybrid polymer/TiO<sub>2</sub> solar cells using poly(ethylenedioxythiophene)/polystyrene sulphonate as hole collector", *Appl. Phys. Lett.*, **86**(14), 143101/1-143101/3, 2005.
14. P. Ravirajan, S.A. Haque, J.R. Durrant, D. Poplavskyy, D.D.C. Bradley, J. Nelson, "Hybrid nanocrystalline TiO<sub>2</sub> solar cells with a fluorine-thiophene copolymer as a sensitizer and hole conductor", *J. Appl. Phys.* **95**, 1473-1480, 2004.
15. S.A. Haque, Y. Tachibana, D. R. Klug, and J. R. Durrant, "Charge Recombination Kinetics in Dye-Sensitized Nanocrystalline Titanium Dioxide Films under Externally Applied Bias", *J. Phys. Chem. B*, **102**, 1745-1749, 1998.
16. P. Ravirajan, A.M. Peiró, M.K. Nazeeruddin, M. Grätzel, J.R. Durrant and J. Nelson, "Hybrid polymer/zinc oxide photovoltaic devices using vertically oriented ZnO nanorods and an ambiphilic molecular interface layer", submitted.